A quiescent prominence observed in the Hα line by the COMP-S instrument at the Lomnický Peak Observatory

P. Schwartz, J. Rybák, A. Kučera, M. Kozák, J. Ambróz and P. Gömöry

Astronomical Institute of the Slovak Academy of Sciences
059 60 Tatranská Lomnica, The Slovak Republic, (E-mail: pschwartz@ta3.sk)

Abstract. A prominence above the NEE limb was observed by the COMP-S instrument attached to the ZEISS coronagraph located at the Lomnický Peak Observatory. Observations were carried out on Nov 2, 2011 between 14:01:13 and 14:11:34 UT. The filter of the instrument was tuned during measurements sequentially in five wavelengths within the profile of the Hα line: 0, ±1, ±2 Å around 6563 Å. FWHM of the transmission function of the filter was ∼0.4Å at these wavelengths. Data were not absolutely calibrated, therefore they could be fitted using only a simple cloud model (1D geometry, a complete frequency redistribution, a source function independent of the optical depth) to diagnose the prominence plasma. As five wavelength points in the profile were not enough for an automatic fitting, five positions at the prominence were chosen for the analysis. Observed data from the five positions were simulated using the cloud model and groups of different models were found for each position. It means that the wavelength scale of a step as large as 1 Å when used for the Hα line is not fine enough for estimation of a correct and unique model. Simulating observations using three different finer wavelength scales it was found that the wavelength scale with a step of 0.3 Å and even more finer in the line core (step of 0.1 Å) is already suitable for more precise and unambiguous plasma diagnostics. We also show that for correct plasma diagnostics it is crucial to take into account an effect of a finite width of the transmission function of the filter. If observed data were fitted irrespectively of this important effect, an error in estimated model parameters could exceed even 100 %, except for the Doppler velocities, for which the error would be much smaller, e.g. for velocities up to $20\,\mathrm{km\,s^{-1}}$ the error is below 1 %.
Key words: Sun – solar prominences – spectroscopy – instrumentation

1. Introduction

Within the past twenty years many new outstanding both space-born or ground--based instruments have been built making possible imaging and spectroscopic observations of solar prominences and/or filaments. For example, UV spectro-scopic observations of the SUMER (*Solar Ultraviolet Measurement of Emitted*

Radiation) spectrograph (Wilhelm *et al.*, 1995) on board of the SoHO (*Solar and Heliospheric Observatory*) satellite were used for non-LTE (where LTE stands for Local Thermodynamical Equilibrium) diagnostics of prominence/filament plasma (see e.g. works of Gunár *et al.* (2010) for a prominence or Schwartz *et al.* (2006) for a filament, and references therein). As spectrographs provide complete line profiles with high spectral resolution, their observations are important for a plasma diagnostics but their disadvantage is that they provide spectra only from positions along a narrow slit at one time and scanning of the larger area takes a rather long time (several tens of minutes). Contrary to this, imaging telescopes can observe a large field of view but in a rather low spectral resolution. For example, Heinzel *et al.* (2008) estimated optical thickness of prominence plasma in four different heights above the solar surface using EUV observations of the TRACE (*Transition Region And Coronal Explorer*) instrument (Handy *et al*, 1999) in a 195 Å channel, X-ray observations by XRT (*X-ray telescope*) and filtergrams in the center of the Hα line by SOT (*Solar Optical Telescope*) on board of Hinode (Kosugi *et al*, 2007). Moreover, there are also instruments capable of observing a larger field of view than a diffraction grating spectrograph and in several wavelength positions in the spectral line profile, such as MSDP (*Multichannel Subtractive Double Pass*) spectrograph (Mein &Bondel , 1972) capable of measuring intensities in several wavelength channels at Hα simultaneously or instruments with tunable narrow-band filters able to scan continuously the whole spectral line profile, such as SOT on Hinode, BBSO Hα telescope, and many others.

The COMP-S (*Coronal multi-channel polarimeter for Slovakia*) instrument mounted on the coronagraph at the Lomnický Peak Observatory belongs to those with tunable filters. The COMP-S is a very powerful and useful instrument capable of scanning in wavelength the whole Hα line and green coronal line (530.28 nm) in all four Stokes profiles taking rather short time and a large field of view. In this work we analyse its first observations of a prominence in the Hα line and adjacent continuum made at five wavelength positions. The observations were made during a comissioning phase of the instrument developement, thus they serve mainly as a test whether the instrument is capable of providing data suitable for the spectroscopic analysis and simulations.

The paper is organised as follows: after the introduction, the COMP-S observations of a prominence and the instrument itself are briefly described. In the third section the results, namely radial velocities, optical thickness at the center of the Hα line and temperatures of the prominence plasma are shown. In Section 4, a wavelength scale for future observations is determined in order to provide data capable of determining unique and correct model providing unambiguous and reliable diagnostics of prominence plasmas. Finally, the last section is Discussion and Conclusions.
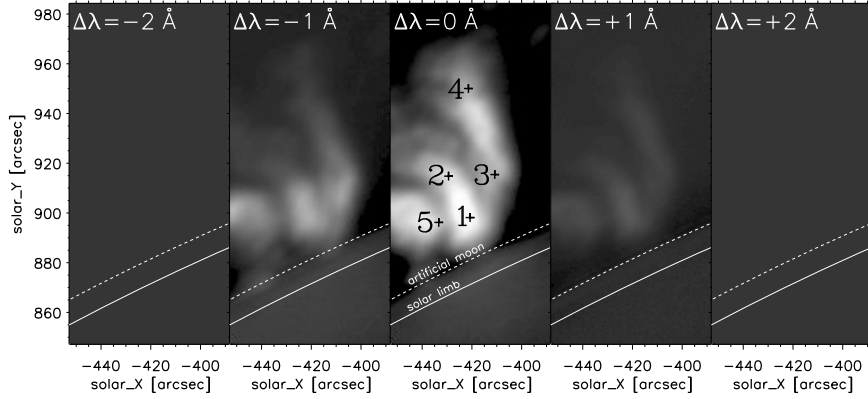
Figure 1. COMP-S observations of the prominence in five wavelength channels at the Hα line: 6563, and 6563±1, 6563±2 Å. Solar X and solar Y are the coordinates according to the disk center.

2. Instrument and observations

The CoMP-S instrument is a 2D multi-channel spectro-polarimeter developed by the HAO/NCAR and installed at the Lomnický Peak Observatory of AISAS (*Astronomical Institute of Slovak Academy of Sciences*) in March 2011 (Kučera et al., 2010). The CoMP-S is attached to the 200/3000 ZEISS coronagraph (Lexa, 1963) as a post-focal instrument with free rotation around the optical axis of the coronagraph. The diameter and focal length of the objective lens of the coronagraph, and the diameter of the resulting solar image (after reimaging optics) are: $D_A = 19.5$ cm, $f = 3$ m and $D_\odot = 4$ cm, respectively. The theoretical spatial resolutions of the coronagraph at the wavelength of 6560 Å is 0.82 arcsec.

The core of the instrument is a Lyot 4-stage filter providing the passband of the FWHM ∼0.4 Å at 6560 Å. The filter is equipped with a polarimeter which allows to measure particular linear combinations of the simple Stokes parameters according to the developed scheme (Tomczyk et al., 2010). Two 16-bit detectors with 2560×2160 of 6.5 micron square pixels are used to acquire light passing in two, slightly shifted in wavelength, spectral passbands tuning one within the emission line profile and the other one to the nearby continuum, respectively.

The particular data used in this paper were acquired early in the commissioning phase of the instrument on Nov 2, 2011 between 14:01:13 and 14:11:34 UT when the height of the Sun above the horizon was very small (only ∼8 degrees) and thus a considerable effect of the terrestrial atmosphere affected the seeing conditions and scattering of the light. Anyway, observed data can be tested on usability for modeling and spectroscopic analysis. And if they are not usable, a correct observing program is to be proposed. The data set is formed by 40 scans of the Hα profile with 5 wavelength points per profile tuned to positions (6563,

and 6563±1, 6563±2 Å). These five filter tunings are hereafter referred to as wavelength channels. The exposure time was 1 s. The FOV was approximately 700×600 arcsec and was located above the NEE limb at the PA ∼75 degrees covering the NOAA AR 11339.

At each wavelength point all 4 frames taken at different combinations of polarizations were added together providing simply the I Stokes intensity parameter with the effective exposure time of 4 s. The dark current and flat field correction of the final Stokes I frames were performed and the continuum was subtracted using data of the extreme wavelength points in each pixel of the FOV. The continuum is formed by scattering of the white-light radiation on free electrons in the solar corona. Light scattered in the Earth's atmosphere and instrument itself also contributes considerably to the continuum intensity. Data were not absolutely calibrated. Observations of the prominence after subtraction of the scattered light in all five wavelength channels are shown in Figure 1. The limb is marked by the white full line, edge of the Lyot stop — the so-called artificial moon — is marked by the dashed line. The profiles from the positions denoted by numbers 1–5 in the middle panel ($\Delta\lambda$=0 Å) were taken for further analysis. The prominence is seen well only in $\Delta\lambda$=0 and −1 Å channels and it is barely visible at +1 Å although this wavelength is already in the continuum. Thus, any radiation of the prominence visible at +1 Å is contributed from wavelengths closer to the line core due to 0.4 Å wide transmission of the filter. Wavelength positions $\Delta\lambda$=±2 Å are already far in the continuum where prominence plasma does not radiate and any radiation at these wavelengths originates from light scattered on free electrons in the solar corona, the Earth's atmosphere and the instrument itself. Therefore, it was correct to subtract the continuum from observations in all five wavelength positions and thus the leftmost and rightmost panels of Figure 1 are totally dark.

3. Modelling observed data using a simple cloud model

As data were not absolutely calibrated, any sophisticated diagnostics using synthetic profiles calculated by a detailed solution of the radiative transfer was not possible. The only possibility is using a simple cloud model where the source function can be taken as a free parameter of the model regardless of physical units in which the intensities are calibrated. When the prominence is approximated by a one dimensional vertically infinite slab irradiated from sides by the solar surface, the intensity $I(\lambda)$ at wavelength λ emergent from the surface of the slab in the line-of-sight direction for a known source function $S(\tau_\lambda)$ can be calculated using the formal solution of the equation of radiative transfer for directional cosine μ equal to 1:

$$I(\lambda) = \int_0^{\tau_\lambda} S(t_\lambda) \exp\left(-t_\lambda\right) dt_\lambda. \tag{1}$$

If the prominence plasma is not optically very thick ($\tau_\lambda \lesssim 1$) at wavelengths of the studied spectral line, then variations of the source function across the slab are negligible, i.e. the source function is independent of the optical depth. For the Hα line this condition is fulfilled for a majority of prominences, as it was already shown by many authors using the detailed solution of the radiative transfer or many different spectroscopic methods, see e.g. Labrosse et al. (2010), Heinzel et al. (2008). Assuming a complete frequency redistribution, what is suitable for the Hα line being a subordinate spectral line, the source function is also independent of wavelength. Then the formal solution (Equation (1)) simplifies as follows:

$$I(\lambda) = S \left[1 - \exp(-\tau_\lambda) \right], \tag{2}$$

while dependence of the optical thickness on wavelength can be defined as follows:

$$\tau_\lambda = \tau_o \, \varphi(\lambda), \tag{3}$$

where τ_o is optical thickness at the profile center λ_C and $\varphi(\lambda)$ is the non--normalized absorption profile. For simplicity, we use a Gaussian profile of the Doppler width $\Delta\lambda_D$ centered at λ_C

$$\varphi(\lambda) = \exp \left[- \left(\frac{\lambda - \lambda_C}{\Delta\lambda_D} \right)^2 \right] \tag{4}$$

because mainly the core of the line is important for our modelling and influence of the Lorentzian profile manifests mainly in the far wings of the profile. Relation between the temperature T and the Doppler width is as follows:

$$\Delta\lambda_D = \frac{\lambda_o}{c} \sqrt{\frac{2kT}{m_H} + v_{mt}^2} \,, \tag{5}$$

where λ_o is the central wavelength of Hα according to some spectral atlas, c is the speed of light, k is Boltzman constant, m_H is the mass of the hydrogen atom and v_{mt} is the velocity of microturbulence. Difference of λ_C from λ_o is taken being due to the Doppler shift. Thus, we defined simple a cloud model with following free parameters: τ_o, λ_C, S, T and v_{mt}. One can see from Equation (5) that the width of the absorption profile is proportional to both the temperature and velocity of microturbulence. For the low mass hydrogen atoms the width is determined mainly by the temperature, although the velocity of microturbulence should not be neglected. For estimation of the v_{mt} velocity, observations of lines of some heavy ions are necessary, for them the width is mainly proportional to the v_{mt} velocity and its dependence on temperature is weaker. Spectral lines of Ca II are widely used for this purpose; namely the H line (Ca II 3968 Å) — can be obtained by an HSFA2 spectrograph (Kotrč, 2009) during joint observing campaigns, or the infrared CaII 8542 Å line — its observations by the COMP-S instrument are in preparation. Unfortunately, we do not have any complementary data in any calcium line for the prominence under study. Thus, reasonable

Table 1. Parameters of the simple cloud models found for COMP-S data in the five chosen points at the prominence as shown in Figure 1. Values of the source function S are in counts after subtraction of scattered light and are expressed in a semi-logarithmic format, i.e. 2.84E5 means 2.84×10^5. More information can be found in the text

position	model name	S [counts]	τ_o	T [K]	Doppl. velocity $[\mathrm{km\,s^{-1}}]$	v_{mt} $[\mathrm{km\,s^{-1}}]$
1	1A	2.84E5	0.5	9 500	-18.0	13
	1B	2.59E5	0.4	17 400	-16.8	13
2	2A	2.59E5	0.3	7 700	-9.6	15
	2B	2.59E5	0.2	9 900	-8.7	15
3	3A	1.13E5	0.8	7 300	-18.4	10
	3B	9.86E4	0.6	13 800	-17.2	10
4	4A	5.43E4	0.6	10 900	-1.9	15
	4B	5.93E4	0.5	8 000	-3.9	15
5	5A	3.30E5	0.2	7 700	-12.5	18
	5B	2.66E5	0.3	13 200	-10.8	18

values of v_{mt} velocity were chosen in order to get temperatures typical for a prominence.

Since we have data only in five wavelength points on a profile, from which two or three are in the continuum, it was not possible to use an automatic fitting of profiles and create maps of parameters of the model. Therefore, we chose five positions in the prominence as shown in the middle panel of Figure 1, and simulated the observed data from these positions. First, observed data were simulated by integration over wavelength of the synthetic profiles multiplied by a Gaussian function of FWHM equal to that of the filter, centered at the five wavelengths that the filter was tuned at. Synthetic profiles were calculated by the so-called basic cloud model chosen by a trial-and-error method in order to get the best agreement between observed and simulated data. Then we calculated extensive catalogues of the simple cloud models for each position at the prominence using values of the microturbulence velocity resulting from the basic models and simulated observed data for each synthetic profile. Finally, we chose a group of models for which absolute values of differences between the simulated and observed data normalized on one data point, are less than 1 % of the maximal intensity of the observed data. In such a way we define agreement of chosen models with observations. Models from the group which are most distant from each other in the space of parameters are denoted A and B. For example, in the left panel of Figure 2 it can be seen that both rather different models A and B agree well with observed data for position 1. The resulting parameters of the models A and B for all five positions (see Figure 1) are shown in Table 1. Instead of the central wavelengths λ_C, corresponding values of the Doppler velocity are listed. The Doppler velocities are calculated using
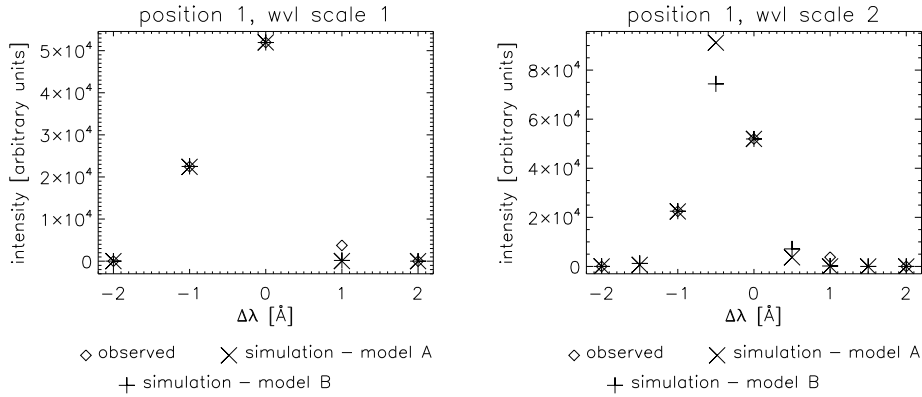
Figure 2. Comparisons of data observed by COMP-S from position 1 with synthetic data obtained for models A and B (named as models 1A and 1B in Table 1) for the wavelength scales 1 and 2 in the left and right panels, respectively. Note the different intensity scales in both panels

a laboratory wavelength of the Hα line center λ_o equal to 6564.68 Å, published by David (1961), as a reference. The positive Doppler velocity is defined for a direction from the observer. For all five positions, there are groups of the models which agree with the observations. The models A and B determine ranges of parameters for models inside the group. Temperatures differing by more than 80 % were estimated in A and B models mainly for data from positions 1, 3 and 5. Differences between other parameters for models A and B are only up to 30 %, only for the Doppler velocity for position 4, the difference between A and B is 105 %. This can be explained by the fact that values of the Doppler velocity estimated for position 4 are rather small and even a small difference between models can lead to a large percentual error. If we simulate observations from synthetic profiles obtained for the models A and B using a finer wavelength scale, simulated data for the models A and B are no longer close to each other, as it is shown in the right panel of Figure 2. In the wavelength positions of scale 2 identical with wavelengths of scale 1, the same intensities for both 1A and 1B models occur. For finer scale 2, new additional intensities are obtained, but they have not been observed. Therefore, we cannot determine which model from the group fits well the observed data. It is Important that the new intensities are different for model 1A and model 1B. Thus, we can conclude, that using a wavelength scale of five points throughout a profile displaced with the step as large as 1 Å, as it was used for observations presented here, it is insufficient for estimations of unique parameters of the simple cloud model. One can suppose that for more sophisticated models the choice of an adequate wavelength scale during observations will be quite crucial.

Thus, the main reason of this work is to find a suitable wavelength scale to obtain as less as possible ambiguous model from the observed data. We solve this task in the next section.

4. A wavelength scale for the Hα line observations suitable for a unique plasma diagnostics

For all five positions chosen at the prominence, the cloud models with parameters in ranges determined by models A and B shown in Table 1 simulate well the Hα data observed at wavelengths ±2, ±1 and 0 Å round 6563 Å (wavelength scale 1). Remarkable differences between models A and B are for temperature which ranges from 30 up to 90 %. In fact, the difference between values of each particular model parameter estimated in model A and model B can be taken as an uncertainty of estimation of the parameter when simulating the observed data. Uncertainties in other parameters are smaller, ranging from several percent up to 20 %, only for the Doppler velocity for position 4 the uncertainty is as big as 101 %.

To test whether observations in a finer wavelength scale can help to obtain acceptable uncertainties of model parameters we took synthetic profiles calculated for all five models A (see Table 1) using the cloud model and simulated observations using the tested scale — i.e. integrating over wavelength the synthetic profiles multiplied by a transmission function of the filter centered at wavelength positions of the scale. Then, we searched in the extensive catalogues of models computed prior to the test for a group of models which differ from simulated observations by less than 1 % at each wavelength position of the scale. Note that also profiles from the catalogues were multiplied by the transmission function and integrated before comparing with the simulated observations. Finally, two models from the group most distant in the parameter space determine the uncertainties. For simulated observations using the wavelength scale 2 — ±2, ±1.5, ±1, ±0.5 and 0 Å, uncertainties of the parameters are much smaller than it was by the wavelength scale 1. Uncertainties in temperature are only up to 15 %. Uncertainties of other parameters do not exceed 10 %. Only for model A for position 1 (the model 1A), the source function smaller by 12 % or the optical thickness τ_{o} larger by 18 % could be estimated. When applying even finer wavelength scale 3 — wavelengths from zero to ±1.5 Å with a step of 0.3 Å, we arrive at uncertainties not exceeding 10 % in temperature, for other parameters maximally 2 %. When assuming errors in measurements of intensities caused by the noise of the CCD camera and by the instrument itself, the uncertainties for wavelength scale 3 are below these errors. Thus, we can assume wavelength scale 3 as suitable for diagnostics using not only the simple cloud model, but also for more sophisticated models based on detailed treatment of the radiative transfer. Note that wavelengths ±2 Å are missing in scale 3, as these wavelengths are already in the far wings of the Hα line observed in the prominence (see the

right panel of Figure 2). The COMP-S instrument is equipped with two cameras; while the first one is observing at the wavelengths tuned by the filter, the second is simultaneously observing at continuum close to the line. Therefore, tuning the filter especially to wavelengths at the continuum is not necessary.

With an increasing value of the optical thickness τ_o, the profile calculated by the cloud model becomes higher and flatter in its core. Contrary to this, the shape of the profile is almost Gaussian for the optical thickness close to zero. With decreasing τ_o, the profile becomes narrower. Therefore, it would be useful to add two wavelength points ± 0.1 to scale 3 and obtain wavelength scale 4 suitable for parts of the prominence with small opacity. When using wavelength scale 4, uncertainties of parameters are similar as at scale 3. For usage of wavelength scale 3 and especially of scale 4 it is important to determine the absolute wavelength at which zero of the scale is located. One can use observed data averaged throughout the whole prominence, estimate the center of an average profile (e.g. by simulating observed data a using simple cloud model). Then the wavelength of the average profile center can be used as the zero position of the wavelength scale. In this case the Doppler velocities relative to average motion of the entire prominence are determined contrary to the values shown in Table 1, where the Doppler velocities were calculated according to the wavelength position of the filter tunned to the Hα center as given by its producer. Another possibility for estimation of the zero of the scale is to observe the edge of the disk close to a prominence and take an average profile, then determine the center of the profile (e.g. by fitting with the Voigt profile) and subsequently use its wavelength as zero of the wavelength scale. In such a case the Doppler velocities relative to the chromosphere close to a prominence are estimated.

5. Discussion and conclusions

It was found that using observations of the Hα line profiles in five wavelength points from interval $\pm 2\,\text{Å}$ with a step of $1\,\text{Å}$ is not suitable for unique diagnostics of the prominence plasma. From Table 1 it can be seen that groups of models in large space of parameters agree with observations. When the step in wavelength becomes as small as $0.5\,\text{Å}$, the uncertainty of estimated temperature is still up to $18\,\%$. Wavelengths relative to the Hα line center as large as $2\,\text{Å}$ are already in the continuum, too far from the emission line. Therefore, the wavelength scale within interval $\pm 1.5\,\text{Å}$ with a step of $0.3\,\text{Å}$ can be suitable for estimations of as unique as possible model. For data from some positions at the prominence — namely 1, 2, and 3 — (see the middle pannel of Figure 1) this scale is capable of providing rather unique diagnostics — uncertainties in the model parameters are below $3\,\%$. For other two positions uncertainties in estimations of the parameters are up to $10\,\%$. A similar wavelength scale with a step of $0.3\,\text{Å}$, but within an interval of $\pm 1.2\,\text{Å}$ and with position at $\pm 0.1\,\text{Å}$ added, enabled diagnostics with

uncertainties below 2% also for these two possitions. The wavelengths $\pm1.5\,\text{Å}$ occurring in the continuum close to the Hα line could be left out from the wavelenegth scale, because the COMP-S instrument observes simultaneosly the spectral line and the continuum (contributed from both white light and light scattered in the Earth's atmosphere and the instrument). Therefore, it is not necessary to tune the filter especially to the continuum. Disadvantage of using these wavelength scales is that the reference wavelength (relative wavelength $0\,\text{Å}$ in the scale) must be estimated prior to the main observations in order to get the wavelength positions $\pm1\,\text{Å}$ in the line core. Thus, we found that observations in the wavelength scale ±1.2, ±0.9, ±0.6, ±0.3, ±0.1 and $0\,\text{Å}$ provide us with more-or-less unique plasma diagnostics. A quite similar wavelength scale is widely used also by the MSDP instrument at Themis or VTT.

Another important criterion for construction of the optimal wavelength scale is whether data observed in this wavelength scale provide us with the correct model parameters when some automatic fitting methods are applied. There is also a question how the noise in the data can influence resulted model parameters. Therefore, we tested our four wavelength scales as follows. We simulated observations using models A for all five positions (see Table 1). Simulated data are synthetic profiles broadened by the filter transmission function measured only in wavelength points of the scale. Then, we added random noise within an interval determined by the Poisson statistics (up to 10%) to the simulted data. Finally, we searched for each simulation, for the best model with the smallest χ^2 in extensive catalogues of models. The catalogues were calculated before the fitting and model profiles were integrated over a transmission function of the filter centered at wavelengths of the wavelength scale. If we arrive by the fitting at similar values of parameters as those used for the simulations of the observations, the wavelength scale can be assumed as suitable. When using wavelength scales 1 or 2, values (estimated by the fitting) of the source function and optical thickness $\tau_{\rm o}$ differ from those used for the simulations by up to 130%. Values of temperature differ by up to 33% and values of the Doppler velocities up to only 5%. For scales 3 and 4 values of the source function and the optical thickness estimated from the fitting differ from those used for simulations already only by up to 44% and the error in estimates of other two parameters does not exceed 10%.

When fitting the observed data using already more sophisticated models or just the simple cloud model, it must be taken into account that observed data were obtained using a filter of a finite width of the transmission function (FWHM of the transmission function of the COMP-S filter $\sim0.4\,\text{Å}$), i.e. measured intensities are specific intensities (the profile of a spectral line) multiplied by a normalized transmission function of the filter and integrated in wavelength. Figure 3 shows comparison of the synthetic profile with simulations of the COMP-S observations calculated using model 1A. For scale 1, simulation points are almost lying on the plot of the synthetic profile. But when using finer wavelength scale 4, simulation points are not lying on the synthetic profile any-
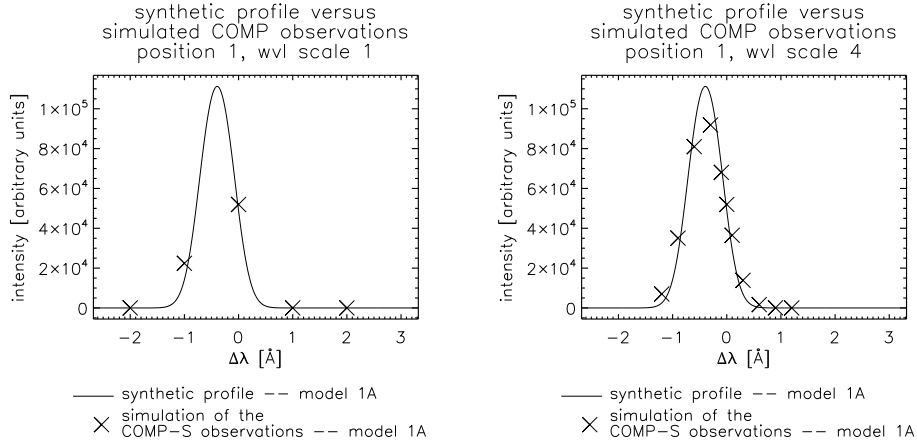
Figure 3. Comparisons of the synthetic profile with simulations of the COMP-S observations calculated using the synthetic profile of model 1A. In the left pannel wavelength scale 1, and in the right panel scale 4 was used.

more, especially in the line core the points are rather far from the profile. Note that if the simulation points would be connected with the curve, they would form a profile that would be broader and lower than the original synthetic profile. This is expectable as the Lyot filter broadens profiles of spectral lines and if we assume that the total energy of a profile does not change, the peak intensity of the filtered profile must be lowered. Only the wavelength position of the profile maximum is not influenced by the filter profile. The question is how large errors in resulting model parameters occur when influence of the transmission function of the filter is neglected. That corresponds in the purely mathematical sense to usage of an infinitesimally narrow transmission function (i.e. the Dirac δ function). We simply fitted simulated data (synthetic data convolved with the filter profile measured at wavelengths of a scale) with synthetic profiles from the catalogue without any multiplication by the transmission function and integration. Then we compared resulted model parameters with the set of parameters used from calculation of the simulated data and evaluated errors. We carried out such a test for all models A ($1A-5A$). The largest error ranging from 100 up to 130% occurs for temperature, errors in the source function and the optical thickness τ_o are of order of $40-80\%$. Errors in estimations of the Doppler velocity are below 1%, which is expectable as convolution with the filter profile does not move the profile maximum. It means that it is possible to estimate correctly only Doppler velocities from the observed data as they are. For correct estimations of other plasma parameters, deconovolution of data from the filter transmission function is necessary prior to modelling. As deconvolution

is numerically and mathematically very complicated and problematic, so-called forward modelling can be used, when response functions of simulated data on the model input parameters are calculated and then they can be used in the numerical fitting method. We will work on this in the near future and this work will be presented in our future papers.

References

David, K.-H.: 1961, *Zeitschrift für Astrophysik* **53**, 37

Gunár, S., Schwartz, P., Schmieder, B., Heinzel, P., Anzer, U.: 2010, *Astron. Astrophys.* **514**, A43

Handy, B. N., Acton, L. W., Kankelborg, C. C., Wolfson, C. J., Akin, D. J., Bruner, M. E., Caravalho, R., Catura, R. C., Chevalier, R., Duncan, D. W., Edwards, C. G., Feinstein, C. N., Freeland, S. L., Friedlaender, F. M., Hoffmann, C. H., Hurlburt, N. E., Jurcevich, B. K., Katz, N. L., Kelly, G. A., Lemen, J. R., Levay, M., Lindgren, R. W., Mathur, D. P., Meyer, S. B., Morrison, S. J., Morrison, M. D., Nightingale, R. W., Pope, T. P., Rehse, R. A., Schrijver, C. J., Shine, R. A., Shing, L., Strong, K. T., Tarbell, T. D., Title, A. M., Torgerson, D. D., Golub, L., Bookbinder, J. A., Caldwell, D., Cheimets, P. N., Davis, W. N., Deluca, E. E., McMullen, R. A., Warren, H. P., Amato, D., Fisher, R., Maldonado, H., Parkinson, C.: 1999, *Sol. Phys.* **187**, 229

Heinzel, P., Schmieder, B., Fárník, F., Schwartz, P., Labrosse, N., Kotrč, P., Anzer, U., Molodij, G., Berlicki, A., DeLuca, E. E., Golub, L., Watanabe, T., Berger, T.: 2008, *Astrophys. J.* **686**, 1383

Kosugi, T., Matsuzaki, K., Sakao, T., Shimizu, T., Sone, Y., Tachikawa, S., Hashimoto, T., Minesugi, K., Ohnishi, A., Yamada, T., Tsuneta, S., Hara, H., Ichimoto, K., Suematsu, Y., Shimojo, M., Watanabe, T., Shimada, S., Davis, J. M., Hill, L. D., Owens, J. K., Title, A. M., Culhane, J. L., Harra, L. K., Doschek, G. A., Golub, L.: 2007, *Sol. Phys.* **243**, 3

Kotrč, P.: 2009, *Central European Astrophys. Bull.* **33**, 327

Kučera, A., Ambróz, J., Gömöry, P., Kozák, M., Rybák, J.: 2010, *Contrib. Astron. Obs. Skalnaté Pleso* **40**, 135

Labrosse, N., Heinzel, P., Vial, J.-C., Kucera, T., Parenti, S., Gunár, S., Schmieder, B., Kilper, G.: 2010, *Space Sci. Rev.* **151**, 243

Lexa, J.: 1963, *Bull. Astron. Inst. Czechosl.* **14**, 107

Mein, P., Blondel, M.: 1972, *Sol. Phys.* **27**, 489

Schwartz, P., Heinzel, P., Schmieder, B., Anzer, U.: 2006, *Astron. Astrophys.* **459**, 651

Tomczyk, S., Casini, R., de Wijn, A.G., Nelson, P.G.: 2010, *Applied Optics* **49**, 3580

Wilhelm, K., Curdt, W., Marsch, E., Schühle, U., Lemaire, P., Gabriel, A., Vial, J.-C., Grewing, M., Huber, M. C. E., Jordan, S. D., Poland, A. I., Thomas, R. J., Kühne, M., Timothy, J. G., Hassler, D. M., Siegmund, O. H. W.: 1995, *Sol. Phys.* **162**, 189